NUCL SCI TECH (2020) 31:66
https://doi.org/10.1007/s41365-020-00776-9

Effects of N-1 substituent on the phototoxicity of fluoroquinolone antibiotics: comparison of pefloxacin and difloxacin

Jian-Feng Zhao[1,2] · Yan-Cheng Liu[1] · Yu-Lie Xu[1,2] · Wen-Feng Wang[1]

Received: 13 March 2020 / Revised: 13 April 2020 / Accepted: 15 April 2020 / Published online: 19 June 2020

Abstract The photophysics and photochemistry of pefloxacin (PEF), a 1-ethyl-substituted fluoroquinolone (FQ) antibiotic, were studied using transient, steady-state experimental methods and computational methods. The fundamental photoproperties of PEF and its phototoxicity toward lysozyme, a single-chain protein, were compared with those of a 1-fluorophenyl-substituted FQ antibiotic, difloxacin (DIF). The results showed that the phototoxicity was significantly decreased by the insertion of the bulky 1-fluorophenyl substituent (the phototoxicity of DIF was approximately one-quarter of that observed for PEF). This trend was attributed to the lowest lying singlet state with sizeable oscillator strength ($f \geq 0.1$) being shifted from 319 nm in PEF to 266 nm in DIF upon the insertion of the bulky substituent at the 1-position, as investigated by using computational methods. In addition, 95% of the solar UV irradiation that reaches the earth's surface has wavelength > 315 nm. Therefore, reducing the most effective excitation wavelength by optimizing the substituent at the 1-position may be a promising strategy to alleviate the phototoxicity of FQ antibiotics. These findings may be applied to other FQ antibiotics because a large number of phototoxicity studies on FQ antibiotics with different substituents at the 1-position can prove these finding's effectiveness. Delafloxacin, an FQ antibiotic bearing a chlorine and bulky substituent at the 8- and 1-positions, respectively, exhibits no phototoxicity is the most recent example reported to date. To the best of our knowledge, this is the first transient and steady-state study of the effect of the N-1 substituent on the photochemistry and phototoxicity of FQ antibiotics. These findings will be beneficial to the development of novel FQ antibiotics without phototoxicity.

Keywords Phototoxicity · FQ antibiotics · Laser flash photolysis · Difloxacin · Pefloxacin · Pulse radiolysis

1 Introduction

The fluoroquinolone (FQ) family of antibiotics comprises hundreds of aromatic compounds that share a similar quinolone structure, and these have been extensively used since they were first applied as clinical therapy [1, 2]. FQ antibiotics have some remarkable advantages, such as broad antimicrobial spectrum, strong antibacterial activity, low rate of drug resistance, and high-cost efficiency [3]. However, they also exhibit some adverse effects [4] that should be eliminated or suppressed.

The adverse effects of FQ antibiotics include dysglycemia, hyperglycemia, tendinitis, central nerve system side effects [5], gene toxicity [6], and phototoxicity [7–11]. Phototoxicity has been reported in most members of the FQ family of antibiotics, and some listed FQ antibiotics have even been discarded due to their severe phototoxic effects

This work was supported by the National Natural Science Foundation of China (No. 21173252).

Electronic supplementary material The online version of this article (https://doi.org/10.1007/s41365-020-00776-9) contains supplementary material, which is available to authorized users.

✉ Wen-Feng Wang
wangwenfeng@sinap.ac.cn

[1] Shanghai Institute of Applied Physics, Chinese Academy of Sciences, Shanghai 201800, China

[2] University of Chinese Academy of Science, Beijing 100049, China

[12], e.g., induction of skin tumors [13]. Therefore, tremendous efforts have been undertaken by the scientific community to unveil the phototoxic mechanism of FQ antibiotics and alleviate their phototoxicity [14].

In general, FQ antibiotics show two types of phototoxicity: (1) direct photosensitization triggered by the excited state of the FQ antibiotic and its subsequent reactivity toward biomolecules and (2) reactive oxygen species (produced via the interaction of ground state oxygen with the excited state FQ antibiotic)-mediated oxidation of biomolecules. The excited state of an FQ antibiotic plays a central role in the two types of phototoxicity displayed by this family of compounds, that is, the characteristics of the FQ antibiotic itself are the dominant factors controlling its phototoxicity. Recent studies have shown that multiple halogen substituents, especially 8-fluorinated derivatives [15], are the main contributors to the severe phototoxicity displayed by FQ antibiotics [12] because the halogen and the aryl radicals generated during the dehalogenation reaction are highly toxic toward biomolecules [16–18]. On the other hand, 8-methoxy-substituted FQ antibiotics, such as gatifloxacin [19] and moxifloxacin [20], are unlikely to exhibit phototoxicity. Although the 8-halogenated substituent has been recognized to be a decisive factor for the phototoxicity exhibited by FQ antibiotics, the structure–phototoxicity relationship is largely unknown due to the complex interactions of the substituents at each position. For example, 8-halogenated FQ antibiotics have been reported to exhibit severe phototoxicity [21], but delafloxacin bearing 8-Cl and 1-(6-amino-3,5-difluoropyridine) groups has been found to be non-phototoxic [22]. Recently, substituents at the 5-position have also been reported to affect the phototoxicity in FQ antibiotics, such as antofloxacin and levofloxacin [23], and the mechanism was unveiled as the combined action of the position and electric effects in our previous research study [24]. 1-ethyl or 1-cyclopropyl FQ antibiotics [25] exhibit severe phototoxicity, whether they contain 8-halogen substituent or not [26]; this important phenomenon has no clear mechanistic explanation and is the origin of the present work. We predict that 1-ethyl and 1-cyclopropyl substituents are capable of attacking the adjacent 8-substituent, especially when the 8-substituent is a halogen, which will facilitate the dehalogenation reaction and the release of halogen and aryl radicals that have been proved to be highly toxic toward biomolecules. This is also the reason we chose a bulky substituent at the 1-position for comparison with 1-ethyl-substituted FQ antibiotics (DIF and PEF). A bulky substituent at the 1-position will hinder the cyclization reaction that connects the 1- and 8- positions as well as suppress the generation of toxic halogen radicals. These controversial results prove the importance of substituent effects and demonstrate the huge challenge toward understanding the structure–phototoxicity relationships of FQ antibiotics.

In this work, pefloxacin (PEF) and difloxacin (DIF), 1-ethyl- and 1-fluorophenyl-substituted FQ antibiotics, were investigated in order to better elucidate the contribution from the substituent effects at the 1-position on the phototoxicity of FQ antibiotics and help clarify the overall scenario of the structure–phototoxicity relationships. The photochemistry of DIF has been previously reported by our group [27]. Therefore, we initially focused on the photochemistry and phototoxicity of PEF in this study, compared its phototoxicity with DIF, and explored the mechanism behind it. The generation of the triplet excimer of PEF ($^3PEF^*$) under laser excitation has also been reported and has been shown to exhibit genotoxic effects [28] due to the formation of thymine cyclobutane dimers via an energy transfer mechanism [29]. However, the interactions of PEF with proteins and its reaction mechanism with DNA/protein under light irradiation as well as a comparison with DIF and the substituent effects at the N-1 position have not been studied to date. The chemical structures and UV–Vis absorption spectra of PEF and DIF are shown in Fig. 1.

2 Experimental

2.1 Materials

PEF (purity > 99.0%) was purchased from J&K Chemical Ltd. DIF (purity > 99.8%), naproxen (NP), 2′-deoxyguanosine-5′-monophosphate (dGMP), and tryptophan (Trp) were purchased from Sigma Chemical Co. All of these compounds met the required purity and were used as received. Sodium dodecyl sulfate polyacrylamide gel electrophoresis (SDS-PAGE) gels were purchased from Life Technologies. tert-Butanol and phosphate salts (analytical grade) were obtained from commercial suppliers and used without further purification. Water was purified using a Millipore-Q system.

2.2 Steady-state absorption measurements

Steady-state UV–Visible absorption experiments were conducted on a Hitachi spectrophotometer (U-3900 type, Japan).

2.3 Determination of the pK_a values

An aqueous solution of PEF at a concentration of 1×10^{-5} mol L^{-1} was prepared. $HClO_4$ and NaOH were utilized to control the pH of the solution, and a glass electrode was employed to monitor the pH. The pK_a values

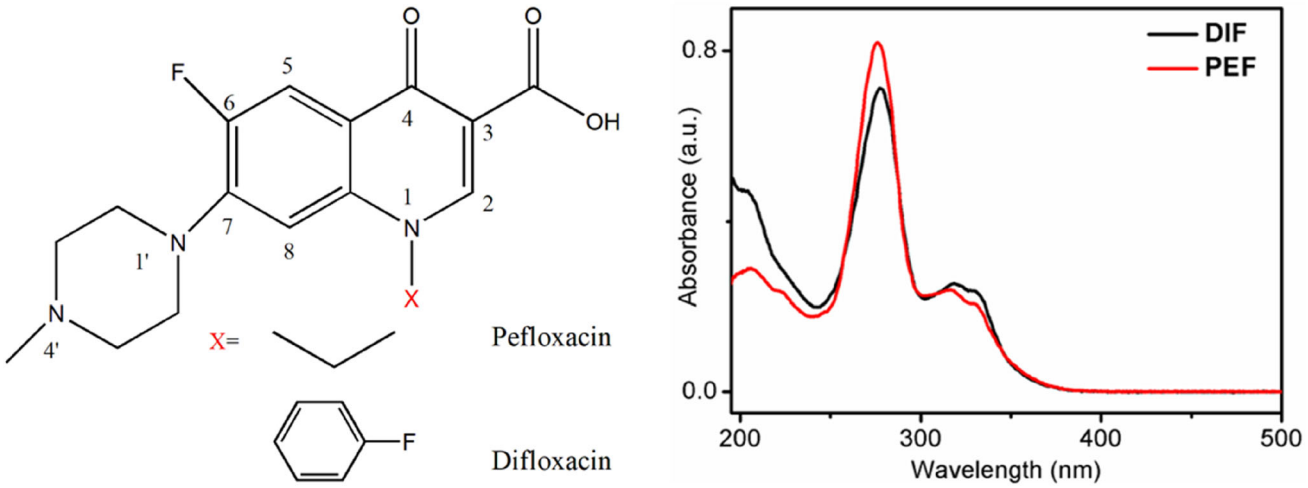

Fig. 1 (Color online) Chemical structures (left) and steady-state UV absorption spectra (right) of pefloxacin (PEF) and difloxacin (DIF) recorded in a neutral aqueous solution

were determined by observing and simulating the half-height of the titration curves.

2.4 Laser flash photolysis (ns-LFP)

An Nd:YAG laser with a wavelength of 355 nm and pulse duration of 5 ns was used as the pump source to conduct our ns-LFP experiments. The energy employed in this work is < 7 mJ per pulse. A detailed description has been provided in our previous report [30]. Unless stated otherwise, the ns-LFP experiments use carefully sealed neutral aqueous solutions saturated with ultrapure N_2 ($> 99.999\%$).

2.5 Pulse radiolysis (ns-PRL)

Ns-PRL experiments were implemented using a linear accelerator [31–34] with 10 MeV energy to generate and transmit an electron pulse, and the duration of each pulse was 8 ns. A detailed description of the ns-PRL setup has been published elsewhere [35].

On the basis of equations (a)–(c) [36], the water molecules are split into several reactive intermediates under the attack of the electron beam, among which, ·OH and e^-_{aq} are the crucial species due to their dominant yield and high reactivity. tert-Butanol was used to scavenge ·OH and e^-_{aq} were retained to create a reducing environment. Conversely, to create an oxidizing environment, N_2O was introduced to saturate sample solution to convert e^-_{aq} into ·OH creating a ·OH radical-dominated oxidizing environment. The influence of the remaining intermediates was negligible under the designed experimental parameters.

$$H_2O \xrightarrow{e^- \text{beam}} OH\cdot,\ e^-_{aq},\ H\cdot,\ H_2,\ H_2O_2,\ HO_2\cdot \quad \text{(a)}$$

$$\cdot OH + \text{tert} - BuOH \rightarrow \text{tert} - BuO\cdot + H_2O \quad \text{(b)}$$

$$k = 5.1 \times 10^8\ \text{dm}^3\ \text{mol}^{-1}\ \text{s}^{-1}$$

$$e^-_{aq} + N_2O + H_2O \rightarrow \cdot OH + OH^- + N_2 \quad \text{(c)}$$

$$k = 8.7 \times 10^9\ \text{dm}^3\ \text{mol}^{-1}\ \text{s}^{-1}.$$

2.6 Sodium dodecyl sulfate-polyacrylamide gel electrophoresis (SDS-PAGE)

A 500-W Xenon lamp was used as the light source. A cutoff filter (centered at 355 nm with a range of 315–375 nm) was used to block light at the undesired wavelengths, which focused the light on a quartz cell with dimensions of $10 \times 10 \times 40\ \text{mm}^3$, yielding an irradiation power of 34.3 mW cm^{-2}. SDS-PAGE (Bio-Rad Mini-PROTEIN® 3 cell) was performed to analyze the freshly irradiated solutions. The gels were stained using the Coomassie method (Coomassie Brilliant Blue G-250 solution) and then destained using a mixed solution of ethanol and ethanoic acid. A Quantity One scanner (Bio-Rad) was employed to evaluate the extent of photodamage [37].

2.7 DFT calculations

Time-dependent density functional theory calculations were conducted at the B3LYP/6-311G* level using the Gaussian 09 program [38].

3 Results and discussion

3.1 Absorption properties

PEF exhibits an intense absorption in an aqueous solution, which consists of two bands (Fig. 2). The molar absorption coefficient (ε_{max}) of the band located at 260–280 nm was determined to be ca. 2.8–4 × 10^4 M^{-1} cm^{-1}, while it was 1.1–1.6 × 10^4 M^{-1} cm^{-1} for the weaker band observed at 310–340 nm. According to the plot of the λ_{max} (310–340 nm) vs pH (Fig. 2, inset), we can see that the data can be modeled using two sigmoidal type curves and the pK_a values were determined to be 5.10 ± 0.02 and 9.20 ± 0.02, respectively (Fig. 3). The structure of PEF contains an alkaline nitrogen atom (the para-N atom in the 7-*N*'-methyl-piperazine ring) and a carboxyl group at the 3-position. This structure enables the zwitterion to be the dominant form in a neutral aqueous solution of PEF. A similar phenomenon was also observed with DIF, and its pK_a values were determined to be 5.91 and 9.89 [27].

According to previous reports [39], the short wavelength band observed at 260–280 nm is caused by the absorption of the aromatic ring, while the long wavelength band at 310–340 nm can be attributed to the $n \rightarrow \pi^*$ (HOMO–LUMO) electronic transition caused by the intermolecular H bond formed between the FQ antibiotic and the solvent (H_2O). The blueshift and decrease in the intensity of the short wavelength band were caused by the dissociation of the 3-carboxylic group when the solution changes from acidic to neutral conditions. We proposed this process based on the results and analysis described above, as shown in Fig. 3.

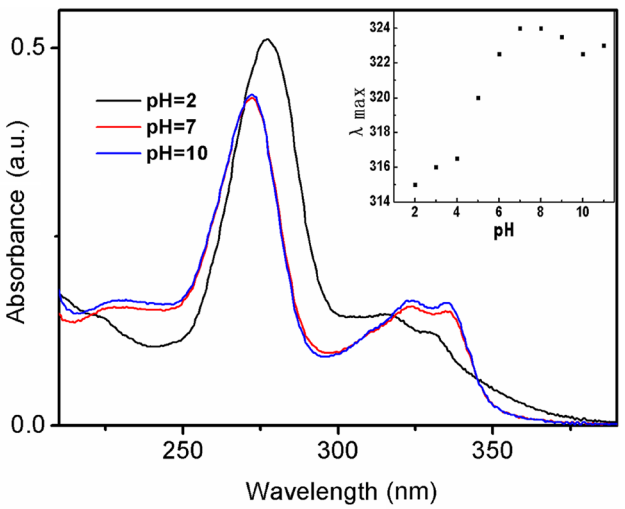

Fig. 2 (Color online) Steady-state absorption spectra obtained for an aqueous solution of PEF under various pH conditions. Inset: plot of λ_{max} vs pH in the wavelength range of 310–340 nm

3.2 Laser flash photolysis (ns-LFP)

Figure 4 shows the time-resolved absorption spectra obtained for a neutral aqueous solution of PEF. The absorption band centered at 610 nm almost disappears within 5 μs; this decay reaction has a rate constant of 6.1 × 10^7 $M^{-1}{\cdot}s^{-1}$. The half-life ($\tau_{1/2}$) of the excited state of PEF in a N_2-purged solution was estimated to be 1.5 μs. However, the decay reaction was significantly accelerated under an oxygen atmosphere with a rate constant of 6.2 × 10^8 M^{-1} s^{-1}, which is one magnitude faster than that observed under a N_2 atmosphere. These results show that the transient species was sensitive to oxygen quenching (Fig. 4, left inset), which is a classic characteristic of a triplet state [40].

The energy transfer quenching pathway proposed in Eq. (1) was applied to verify that the aforementioned excited state of PEF is a triplet state ($^3PEF^*$) and was used to estimate the energy of $^3PEF^*$. Since the λ_{max} of $^3NP^*$ is centered at ~ 430 nm [41] and its triplet energy is 259 kJ mol^{-1} based on Eq. (2) (Sandros equation), the reaction rate constant (k_{ET}) is only dependent on the triplet energy gap (ΔE_T) between $^3PEF^*$ and $^3NP^*$. The k_{max} in Eq. (2) is the optimized rate constant for FQ antibiotics and NP, which was assumed to be 2.2 × 10^9 M^{-1} s^{-1}. It is the average value of this diffusion controlled energy transfer reaction between the triplet excited state of some FQ antibiotics and the ground state of NP [29]. Therefore, the triplet energy of $^3PEF^*$ can be estimated by tracking its decay–time dependence during the energy transfer process.

$$^3PEF^* + NP \rightarrow {}^3NP^* + PEF \quad (1)$$

$$k_{ET} = k_{max} \times \frac{\exp\left(-\frac{\Delta E_T}{RT}\right)}{1 + \exp\left(-\frac{\Delta E_T}{RT}\right)} \quad (2)$$

Figure 5 shows that at the end of the laser pulse, a new band was detected at ~ 610 nm, which then decayed to form a new band at 430 nm. As mentioned beforehand, the band at 430 nm can be assigned to $^3NP^*$ and thus confirms the excited state of PEF was $^3PEF^*$; the k_{ET} value was estimated to be 1.66 × 10^9 $M^{-1}{\cdot}s^{-1}$ (Fig. 5, right inset). Hence, the triplet energy gap (ΔE_T) between $^3PEF^*$ and $^3NP^*$, and the energy of $^3PEF^*$ was calculated as 6 and 265 kJ mol^{-1}, respectively, according to Eq. (2), which is in good agreement with those reported in the literature (269 kJ mol^{-1}) [29].

The reactions of $^3PEF^*$ with Trp and dGMP were investigated in order to study the reactivity of $^3PEF^*$ and its capability toward oxidizing biomolecules, including nucleic acid and amino acids. Trp is one of the most feasible sites for protein oxidation [42] and dGMP is a well-established model compound of DNA [43]. Hence, their oxidation can be treated as an indicator of the

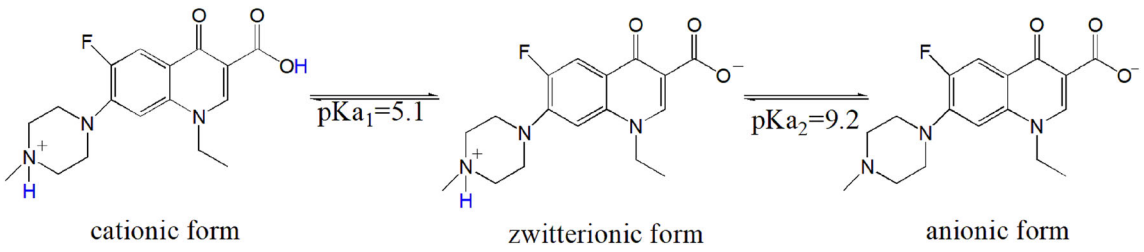

Fig. 3 Equilibrium formed among various protonated forms for PEF

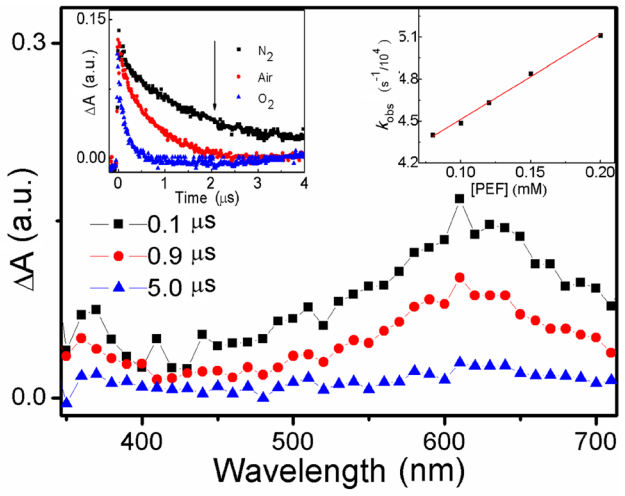

Fig. 4 (Color online) Time-resolved absorption spectra observed at (filled square) 0.1 μs, (filled circle) 0.9 μs, and (filled triangle) 5.0 μs after photoexcitation of an ultrapure nitrogen-saturated solution of PEF (0.2 mM). Inset: (left) the decay–time curves observed for PEF (0.2 mM, pH = 7.1) under different atmospheres; (right) the relationship between the apparent decay rate constants observed at 610 nm (k_{obs}) and the concentration of PEF ([PEF])

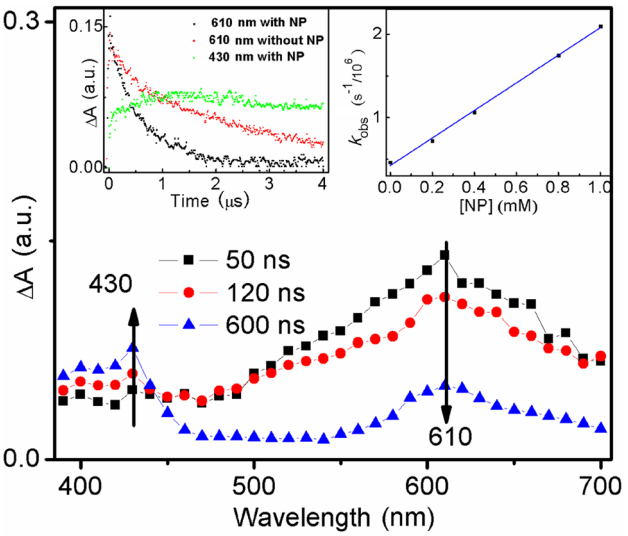

Fig. 5 (Color online) Time-resolved spectra obtained for a solution of PEF (0.1 mM) and NP (0.5 mM) at different delay times of (filled square) 50 ns, (filled circle) 120 ns, and (filled triangle) 600 ns after optical excitation. Inset: (left) the generation and decay–time curves monitored at 430 and 610 nm; (right) the curves obtained for k_{obs} vs NP (energy acceptor and quenching reagent) used to determine the apparent rate constants at 610 nm

photosensitive damage to biomolecules. The triplet energy of dGMP is 317 kJ mol^{-1} [44], which is much higher than that calculated for $^3PEF^*$(265 kJ mol^{-1}). Therefore, it is unlikely to transfer energy from $^3PEF^*$ to dGMP. The transient absorption spectra obtained for a mixed solution of PEF and dGMP are shown in Fig. 6. On this occasion, PEF was excited to generate its corresponding triplet state ($^3PEF^*$) and the direct excitation of dGMP can be neglected due to its extremely low absorption at this wavelength [45]. This was further confirmed using a blank experiment, i.e., no absorption band was observed in the laser flash photolysis study using a neutral aqueous solution of dGMP under the same experimental conditions. The absorption band was instantly formed upon optical excitation, which decayed faster upon increasing the concentration of dGMP (Fig. 6, left inset). A band centered at 370 nm clearly emerged upon the decay of $^3PEF^*$. The absorption band of the dGMP cation radical ($dGMP^{+\cdot}$) is located at 310 nm [46]; however, in the present work, the absorption band corresponding to $dGMP^{+\cdot}$ was not observed due to the strong ground state bleaching of PEF in the range of 310–350 nm. Nevertheless, the transient absorption of the PEF radical anion ($PEF^{-\cdot}$) was confirmed at 370 nm in our pulse radiolysis study, which will be discussed in the following section. Furthermore, the electron transfer observed from dGMP to ciprofloxacin, an analogue of PEF, has been unambiguously proved [10] and energy transfer pathway was excluded. Therefore, it is reasonable to conclude that the accelerated decay of $^3PEF^*$ in the presence of dGMP can be attributed to the electron transfer reaction between dGMP and $^3PEF^*$. We also determined the rate constant of the reaction to be 2.8×10^7 M^{-1} s^{-1} (Fig. 6, right inset).

We found that $^3PEF^*$ can be quenched by Trp in a similar way. The quenching process of $^3PEF^*$ is significantly accelerated with a quenching rate constant of 6.3×10^7 M^{-1} s^{-1} upon the addition of Trp (Fig. 7, right inset). The absorption band observed at $\sim$ 660 nm was assigned as hydrated electrons, which can be used as

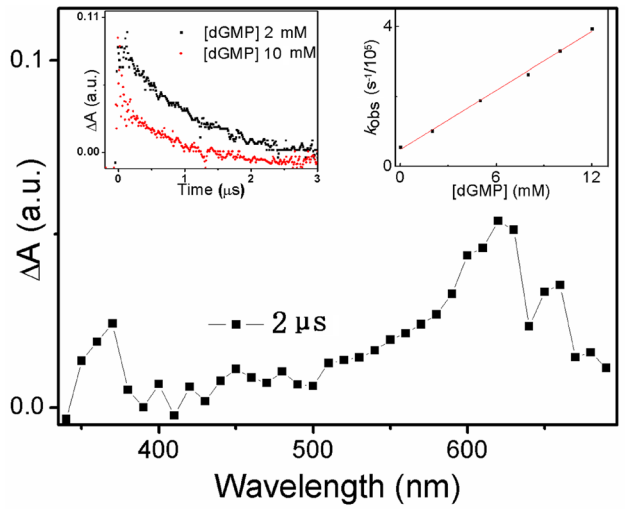

Fig. 6 (Color online) Transient absorption spectra recorded 2 μs after optical excitation for solutions containing PEF (0.1 mM) and dGMP (5 mM), respectively. Inset: (left) the absorbance–time profile tracked at 610 nm using different concentrations of dGMP; (right) the relationship between the rate constant (k_{obs}; 610 nm, $^3PEF^*$) and concentration of dGMP ([dGMP])

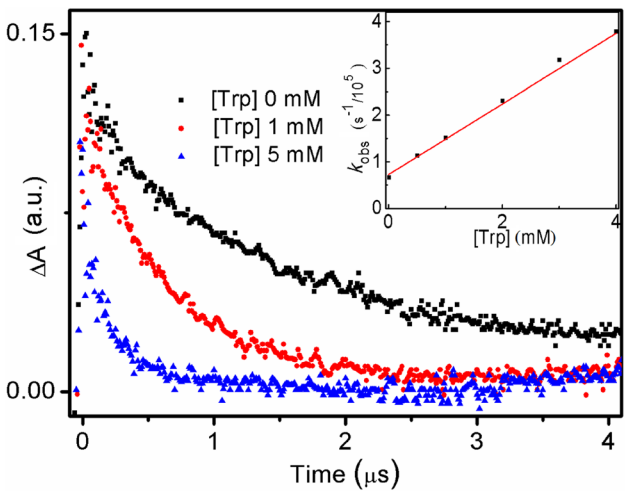

Fig. 7 (Color online) Absorbance–time curves obtained at 610 nm after optical excitation of a 0.1 mM solution of PEF containing 0, 1, and 5 mM Trp, respectively. Inset: plot of the $^3PEF^*$ apparent decay rate constant observed at 610 nm (k_{obs}) vs the concentration of Trp ([Trp])

evidence for the occurrence of the electron transfer reaction between $^3PEF^*$ and dGMP. According to the results and analysis described beforehand, the electron transfer reactions between $^3PEF^*$and dGMP (or Trp) can be described using Eqs. (3) and (4).

$$^3PEF^* + dGMP \rightarrow dGMP^{\cdot+} + PEF^{\cdot-} \quad (3)$$

$$^3PEF^* + TrpH \rightarrow Trp^{\cdot} + H^+ + PEF^{\cdot-} \quad (4)$$

3.3 Pulse radiolysis (ns-PRL)

To confirm the species generated from PEF and dGMP at 370 nm was $PEF^{\cdot-}$, an ns-PRL experiment using PEF with hydrated electrons (e^-_{aq}) was carried out, as shown in Fig. 6. In consideration that $^{\cdot}OH$ is the dominant reactive species formed during the degradation of FQ antibiotics [47] and the potential photoionization of $^3PEF^*$ may also produce the radical cation of PEF ($PEF^{\cdot+}$) via photoionization, which can be compared with the electron transfer reaction between PEF and $^{\cdot}OH$, the reaction of PEF with $^{\cdot}OH$ was also investigated.

3.3.1 Reaction with hydrated electrons (e^-_{aq})

Ns-PRL experiments were performed using an ultrapure nitrogen-saturated mixed neutral solution containing phosphate (2 mM), t-BuOH (2 mM), and PEF (0.2 mM) in order to investigate the anion radical generated from PEF ($PEF^{\cdot-}$). In this system, both $^{\cdot}OH$ and e^-_{aq} radicals can be generated due to the attack of water molecules by the high energy electron beam, in which $^{\cdot}OH$ was then eliminated upon reaction with t-BuOH, as shown in Eq. (b). Therefore, under these experimental conditions, the obtained signals can be assigned to the reduction in PEF by e^-_{aq}. The transient spectra of e^-_{aq} have a characteristic broad band observed from 450 to 730 nm. However, a growth followed by decay profile was observed at 370 nm for PEF, which is obviously different from the simple decay profile observed for the blank experiment (Fig. 8, Inset, left). Thus, the maximum transient absorption of $PEF^{\cdot-}$ can be assigned as

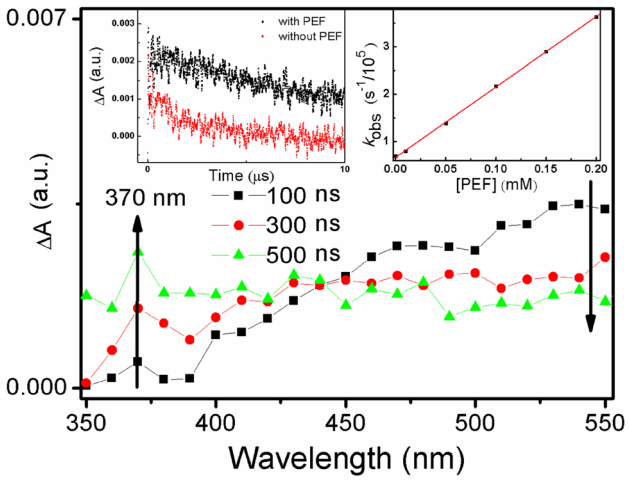

Fig. 8 (Color online) Time-resolved absorption spectra observed for a solution of PEF (0.2 mM) at different time delays after being bombarded by an electron beam under a N_2 saturated atmosphere. Inset: (left) the decay–time curves observed for the solution containing PEF (filled square) and without PEF (filled circle) at 370 nm; (right) the relationship between the e^-_{aq} apparent reaction constant observed at 690 nm (k_{obs}) and concentration of PEF ([PEF])

the band observed at 370 nm. The reaction constant (1.5×10^{10} $M^{-1}{\cdot}s^{-1}$) was estimated for the reaction between PEF and e^-_{aq} by tracking the decay of band at 690 nm against the concentration of PEF. On account of these results, the process of this reaction was proposed using Eq. (5).

$$e^-_{aq} + PEF \rightarrow PEF^{\cdot -} \quad (5)$$

3.3.2 Reaction with ·OH

If the system is a N_2O-purged mixed neutral solution of PEF (0.1 mM) and phosphate buffer (PB, 2 mM), then after ns-PRL the ·OH will be the primary reactive radical according to Eq. (c). The time-resolved spectra obtained 2.0 μs after the electron pulse are displayed in Fig. 9, and the rate constant between ·OH and PEF was deduced from the curve generated from the absorption band centered at 410 nm, which was estimated to be 6.5×10^9 M^{-1} s^{-1}. This value is reasonable because most aromatic compounds react with ·OH with rate coefficients in the range of 6–8×10^9 M^{-1} s^{-1} [48]. It is known that ·OH reacts with aromatic molecules via three different pathways: addition, hydrogen abstraction, and electron transfer [49]; therefore, we attempted to identify the dominant reaction pathway between ·OH and PEF. The computational absorption spectra for the addition ($[PEF\text{-}OH]^{\cdot}$), H-abstraction ($(PEF(-H)^{\cdot}$, and electron transfer ($PEF^{+\cdot}$) products were calculated and compared with the experimental absorption spectra. Unfortunately, none of them was in accordance with experimental results. On the contrary, a mixture of these three products was better suited to the experimental spectra (data not shown). Using the time-resolved spectra and computational calculations, the mechanism of ·OH and PEF was proposed, as shown in Eqs. (6)–(8):

$$PEF + \cdot OH \rightarrow PEF^{\cdot +} + OH^- \quad (6)$$

$$PEF + \cdot OH \rightarrow [PEF{-}OH]^{\cdot} \quad (7)$$

$$PEF + \cdot OH \rightarrow [PEF{-}H]^{\cdot} + H_2O \quad (8)$$

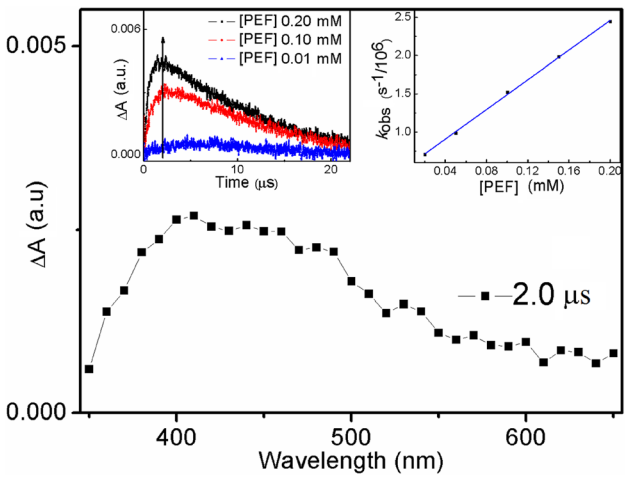

Fig. 9 (Color online) Time-resolved absorption spectrum obtained for the transient species in a N_2O purged neutral solution of PEF (0.2 mM) recorded 2 μs after being bombard by the electron pulse. Inset: (left) the generation–time profiles obtained with PEF at 410 nm [(filled square) 0.20 mM, (filled circle) 0.10 mM, and (filled triangle) 0.01 mM]; (right) the apparent formation rate constants (K_{obs}) observed at 410 nm versus the concentration of PEF ([PEF])

3.4 SDS-PAGE

3.4.1 The effects of the irradiation time and concentration

The gel electrophoresis results obtained using an aqueous solution of lysozyme (M.W. = 14.4 kDa [50] and constant concentration) containing different concentrations of PEF at various illumination times are shown in Fig. 10. The band intensity at 28–31 kDa is recognized as the dimer of the lysozyme monomers bound via Trp-Trp cross-links [51, 52]. The number of Trp-Tyr and Tyr-Tyr cross-links [53] increases significantly upon increasing the concentration of PEF and illumination time. These results can be rationally explained by both the longer illumination time and higher concentration of PEF resulting in a higher proportion of the excited states of PEF, which effectively react with Trp and generate the neutral radical of Trp via Eq. (4) as discussed beforehand, thus increasing the crosslinking of lysozyme.

3.4.2 A comparison of the phototoxicity of DIF and PEF

Because the phototoxicity of PEF has been confirmed in this work and the reaction between DIF and biomolecules has been previously reported [27], it is reasonable to assume that a comparison of the phototoxic effects of these FQ antibiotics will be useful toward unveiling the substituent effects at the 1-position. Aqueous solutions of lysozyme containing DIF and PEF with the same absorption intensity at 355 nm (OD_{355nm} = 0.20) were illuminated, and the intensity of the dimers and trimers was compared with the blank sample. Figure 10 shows that under the same experimental conditions, the intensity of the dimers in the sample containing DIF increased slightly when compared with the blank sample, which suggests the weak phototoxicity of DIF. On the contrary, the intensity of the dimers in the sample containing PEF was much stronger. More specifically, the enhanced phototoxic effect brought by PEF (38.0%) was fourfold higher than that observed for DIF (9.2%, calculated from Fig. 11b). This result was in accordance with the conclusion of a previous study stating that the phototoxicity of PEF is comparable to lomefloxacin [54], a well-known phototoxic FQ antibiotic

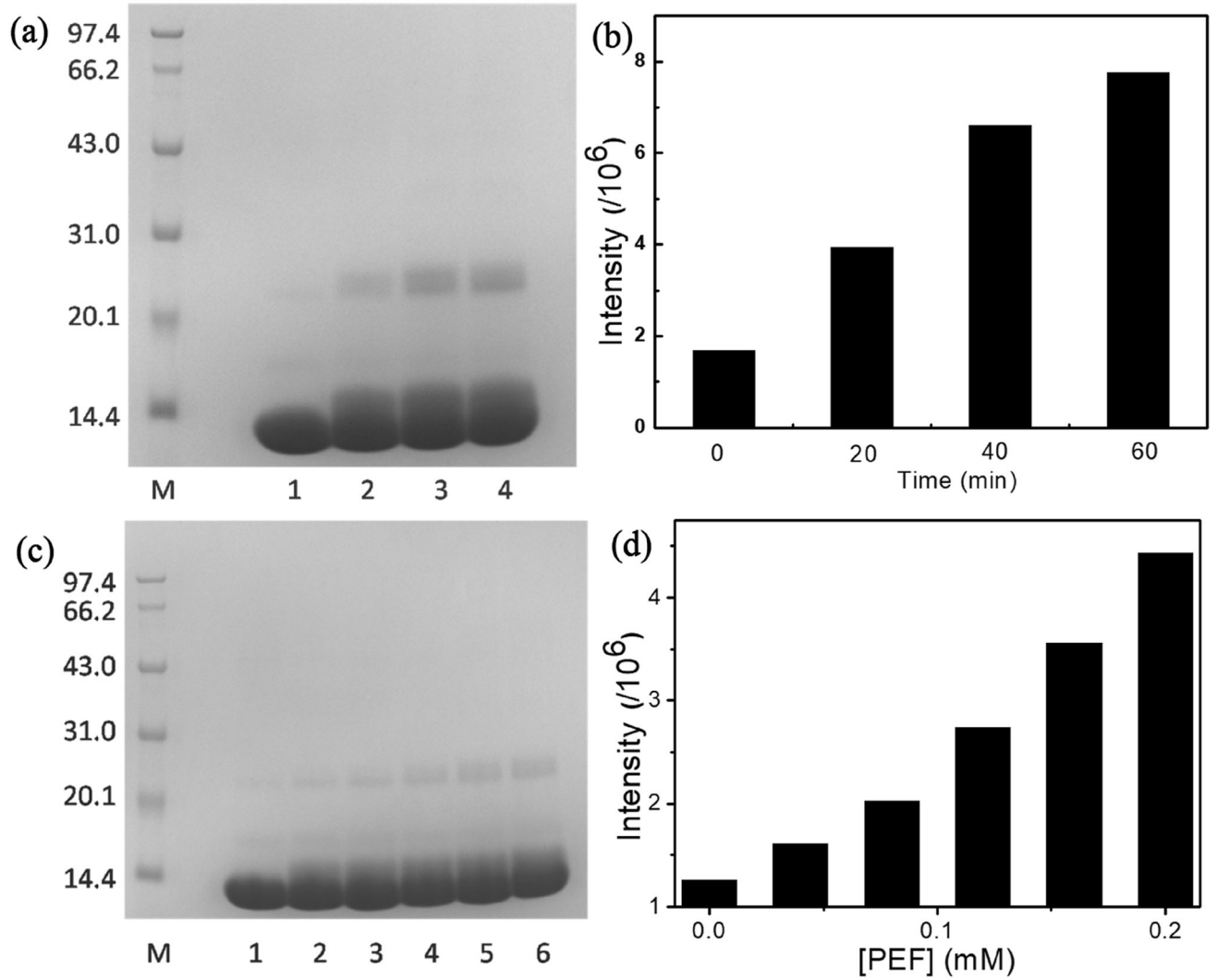

Fig. 10 Patterns obtained using gel electrophoresis unveil the effect of the **a** irradiation time and **c** PEF concentration on the degree of photodamage to lysozyme caused by PEF. M: marker of molecular weight. **b** Intensity of bands extracted from dimer bands (28–31 kDa), lysozyme (0.5 mM), PEF (0.20 mM), air bubbling for 0, 20 min, 40, and 60 min. **d** Intensity of bands extracted from dimer bands (28–31 kDa), 0.5 mM lysozyme, air bubbling for 30 min at a PEF concentration of 0, 0.04, 0.08, 0.12, 0.16, and 0.20 mM, respectively

[55]. This is also in agreement with the reported phenomenon that 1-ethyl FQ antibiotics will be phototoxic no matter if the 8-position is halogenated or not [26].

Why do 1-ethyl FQ antibiotics exhibit severe phototoxic effects when compared with 1-fluorophenyl FQ antibiotics? To answer this, we should firstly review the mechanisms of their phototoxicity. There are two general types of photosensitization pathway observed for the photooxidation of biomolecules. Type I is the direct interaction between the excited photosensitizer (or photoexcited degradation products of the original photosensitizer) and biomolecules, while type II is the energy transfer reaction from the excited photosensitizer to ground state molecular oxygen (O_2, triplet) to produce singlet oxygen ($^1O_2$), followed by $^1O_2$-mediated oxidation of the biomolecule [56]. The excited states of the photosensitizer (photoexcited PEF and DIF molecules) can be a singlet state, but more commonly, they are dominated by excited triplet states [57] due to the significantly longer life time of the triplet state.

Following these mechanisms, we systematically analyzed and compared the processes after the photoexcitation of PEF and DIF. The fundamental photoproperties related to PEF and DIF are displayed in Table S1 in the Supporting Information. We first analyzed the type I mechanism, which involves the excited singlet and triplet states of PEF and DIF, as well as potential secondary photosensitizers that are generated by the photodegradation of the singlet and triplet states of PEF and DIF. As shown in Fig. 1, PEF and DIF belong to 4′-*N*-alkylated FQ antibiotics and their primary pathway of photodegradation is the demethylation

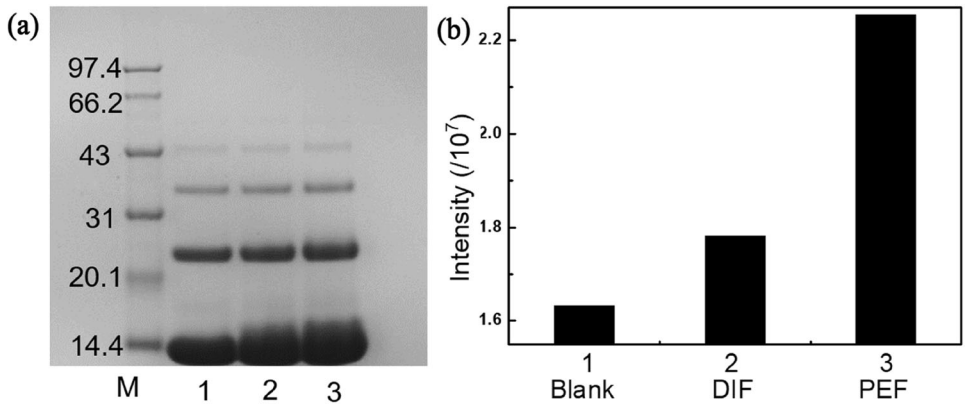

Fig. 11 **a** Patterns obtained using gel electrophoresis illustrates the phototoxic effect of DIF and PEF. **b** Intensity of bands extracted from dimer bands (28–31 kDa). Air bubbling: (1) lysozyme (blank control), (2) lysozyme + DIF, and (3) lysozyme + PEF with illumination for 40 min. M: molecular weight marker. Measured at the same OD ($OD_{355\ nm}$ = 0.20) of DIF and PEF in a neutral aqueous solution containing 0.5 mM lysozyme

reaction [58, 59], in which the products are also two phototoxic FQ antibiotics, norfloxacin (NOR) and sarafloxacin (SAR) (Fig. S1), respectively. So the excited states of PEF and DIF, and their photoproducts should be compared separately.

Firstly, the ground states of PEF and DIF will be excited to their singlet states upon illumination with light. Based on the time-dependent density functional theory (TD-DFT) calculations performed at the B3LYP/6-311G* level of theory (Gaussian 09 program), the excited singlets of PEF and DIF with the lowest energy were almost the same (3.09 and 3.11 eV at 401 and 398.5 nm, respectively) and this calculation was also in accordance with the UV–Vis absorption spectra obtained for PEF and DIF, as shown in Fig. 1, which are almost identical at longer wavelengths. However, singlet states with both the lowest energy and sizeable oscillator strength ($f \geq 0.1$) [60] were observed at 318.9 nm (3.89 eV) and 266.2 nm (4.66 eV) for PEF ($f = 0.114$) and DIF ($f = 0.463$), respectively (Table S2 and S3). The much lower energy of the singlet states with sizeable oscillator strength indicates the higher probability to transfer from the ground state to their corresponding excited singlet states. This suggests that the excited singlet generation process was much more feasible for PEF than DIF under UVA (315–400 nm) irradiation. Furthermore, > 95% of sunlight that arrives at the earth's surface is located in the UVA region [61], which will facilitate the generation of singlet PEF (^{1}PEF*), but not the generation of singlet DIF (^{1}DIF*).

Secondly, except for the direct reaction with biomolecules, which should be negligible due to the rapid decay of the singlet states ($\tau \leq 10^{-9}$ s) [60], the generated ^{1}PEF* and ^{1}DIF* can transform into their triplet states via an intersystem crossing (ISC) process or photodegradation reaction, both of which can contribute to photosensitive damage. The lifetime of these singlet states is too short to trigger photosensitive damage, and thus, there is no need to consider their direct contribution in this work. Table S1 shows the energy difference between ^{3}PEF* and ^{3}DIF*, 1.5 kJ·mol^{-1}, which is insignificant, while the quantum yield of the intersystem crossing process (Φ_{ISC}) for PEF was 1.6-fold higher than that of DIF while the rate constant with biomolecules for DIF was approximately threefold higher than that observed for PEF. The higher rate constants indicate that DIF displays phototoxicity faster than PEF, but it is not the reaction rate that acts as the decisive factor in the severity of the phototoxicity because in the present work the value observed for lysozyme is 2.5-fold higher than that of the FQ antibiotics and one lysozyme molecule contains six reactive Trp residues [62], which offers enough oxidation sites for the photoexcited FQ antibiotic molecules. Furthermore, the biomolecules found in humans or animals are also found in excess when compared with the number of photosensitizers that exist in their body. The quantum yield of the triplet state of the photoproduct of PEF (NOR, $\Phi'_{ISC} = 0.52$) was also 1.5-fold higher than that observed for DIF (SAR, $\Phi'_{ISC} = 0.35$, Table S1). The lower quantum yield observed for ^{3}SAR* was similar to ^{3}DIF* because the bulky substituent in the1-position remains the same in SAR as that observed in DIF.

As for the type II mechanism, according to previous studies, the quantum yields of singlet oxygen for PEF, DIF, and their primary degradation products, NOR [63] and SAR [64], are comparable and as low as 0.06–0.10 in a neutral aqueous medium [54]. Therefore, the type II mechanism is not important when comparing the phototoxicity of PEF and DIF.

In one word, the insertion of a bulky substituent at the 1-position gives rise to a significant increase in the energy gap between the ground state and the lowest sizeable

excited singlet state of FQ antibiotics, which further results in the lower quantum yield of their triplet states and lower phototoxicity.

This proposed mechanism may be applied to the whole family of FQ antibiotics because it has been proved using several other FQ antibiotics. To name a few, SAR, a 1-fluorophenyl FQ antibiotic, also has lower Φ_{ISC} and weaker phototoxicity than that of its counterpart NOR, a 1-ethyl FQ antibiotic. Moreover, it has been confirmed using several phototoxicity studies on other FQ antibiotics with various substituents at the 1-position [22, 26, 65], among which delafloxacin, a newly listed FQ antibiotic bearing a Cl and bulky substituent at the 8- and 1-position, respectively, has been shown to be free of phototoxicity [22]. FQ antibiotics bearing a halogen substituent at the 8-position usually exhibit broader antibacterial activity, improved oral bioavailability, but they are rarely commercialized due to their severe phototoxicity. The use of a bulky substituent at the 1-position may dramatically reduce the phototoxicity of FQ antibiotics and will be a promising synthetic strategy for the development of the next generation of FQ antibiotics.

4 Conclusion

Herein, the photochemistry and phototoxicity of PEF, a 1-ethyl-substituted FQ antibiotic, have been investigated and compared with its counterpart, DIF, a 1-fluorophenyl FQ antibiotic. The insertion of a bulky substituent at the 1-position enables the absorption band of the lowest sizeable ($f \geq 0.1$) singlet to be blueshifted from 319 nm (PEF) to 266 nm (DIF) and decreases the quantum yield of their excited triplet states to some extent, which are the crucial intermediates in the photosensitization process and thus significantly reduce their phototoxicity. To the best of our knowledge, this is the first study combining transient, steady-state, and computational methods based on different substituents located at the 1-position of FQ antibiotics and proposes a mechanism of why the insertion of a bulky substituent at the 1-position can alleviate the phototoxicity. This study will be beneficial to the development of novel FQ antibiotics that are free of phototoxicity.

Acknowledgements The authors thank Dr. Xing-Xing Jiang from the Technical Institute of Physics and Chemistry, Chinese Academy of Sciences, and Dr. Xiting Zhang from the University of Hong Kong for their advice on our DFT calculations.

References

1. O. Cars, S. Molstad, A. Melander, Variation in antibiotic use in the European Union. Lancet **357**(9271), 1851–1853 (2001). https://doi.org/10.1016/S0140-6736(00)04972-2
2. A.I. Nabeel, F.S.M. Moawed, H. Hassan, Immunomodulatory effect of new quinolone derivative against cisplatin/gamma radiation-induced renal and brain toxicity in mice. J. Photochem. Photobiol. B **184**, 54–60 (2018). https://doi.org/10.1016/j.jphotobiol.2018.05.013
3. I.A. Dhalla, M.M. Mamdani, A.E. Simor et al., Are broad-spectrum fluoroquinolones more likely to cause Clostridium difficile-associated disease? Antimicrob. Agents Chemother. **50**(9), 3216–3219 (2006). https://doi.org/10.1128/AAC.00592-06
4. P.C. Appelbaum, P.A. Hunter, The fluoroquinolone antibacterials: past, present and future perspectives. Int. J. Antimicrob. Agents **16**(1), 5–15 (2000). https://doi.org/10.1016/S0924-8579(00)00192-8
5. G. Schmuck, A. Schurmann, G. Schluter, Determination of the excitatory potencies of fluoroquinolones in the central nervous system by an in vitro model. Antimicrob. Agents Chemother. **42**(7), 1831–1836 (1998). https://doi.org/10.1128/AAC.42.7.1831
6. A. Zgadzaj, J. Kornacka, A. Jastrzebska et al., Development of photoprotective, antiphototoxic, and antiphotogenotoxic formulations of ocular drugs with fluoroquinolones. J. Photochem. Photobiol. B **178**, 201–210 (2018). https://doi.org/10.1016/j.jphotobiol.2017.11.011
7. E. Rubinstein, History of quinolones and their side effects. Chemotherapy **47**, 3–8 (2001). https://doi.org/10.1159/000057838
8. Y.L. Xu, Y.C. Liu, F.J. Zhao et al., Photochemical properties of gemifloxacin: a laser flash photolysis study. J. Photochem. Photobiol. B **143**, 30–37 (2015). https://doi.org/10.1016/j.jphotobiol.2014.12.014
9. Y.L. Xu, Y.C. Liu, H.X. Li et al., Photosensitive damage of lysozyme caused by pazufloxacin and the protective effect of ferulic acid. Sci. China Chem. **58**(3), 508–513 (2015). https://doi.org/10.1007/s11426-014-5174-z
10. Y.C. Liu, P. Zhang, H.X. Li et al., Ciprofloxacin photosensitized oxidation of 2'-deoxyguanosine-5′-monophosphate in neutral aqueous solution. Photochem. Photobiol. **88**(3), 639–644 (2012). https://doi.org/10.1111/j.1751-1097.2012.01092.x
11. Y.C. Liu, P. Zhang, H.X. Li et al., Photochemical properties and phototoxicity of Pazufloxacin: a stable and transient study. J. Photochem. Photobiol. B **118**, 58–65 (2013). https://doi.org/10.1016/j.jphotobiol.2012.11.002
12. P. Ball, Adverse drug reactions: implications for the development of fluoroquinolones. J. Antimicrob. Chemother. **51**, 21–27 (2003). https://doi.org/10.1093/jac/dkg209
13. G. Klecak, F. Urbach, H. Urwyler, Fluoroquinolone antibacterials enhance UVA-induced skin tumors. J. Photochem. Photobiol. B **37**(3), 174–181 (1997). https://doi.org/10.1016/S1011-1344(96)07424-6
14. W.B. Kim, A.J. Shelley, K. Novice et al., Drug-induced phototoxicity: a systematic review. J. Am. Acad. Dermatol. **79**(6), 1069–1075 (2018). https://doi.org/10.1016/j.jaad.2018.06.061
15. M. Freccero, E. Fasani, M. Mella et al., Modeling the photochemistry of the reference phototoxic drug lomefloxacin by steady-state and time-resolved experiments, and DFT and post-HF calculations. Chem. Eur. J. **14**(2), 653–663 (2008). https://doi.org/10.1002/chem.200701099
16. T. Su, M.D. Li, J.N. Ma et al., Time-resolved spectroscopic study of the defluorination and cyclization reactions of lomefloxacin in water. J. Phys. Chem. B **121**(17), 4512–4520 (2017). https://doi.org/10.1021/acs.jpcb.6b11267

17. B. Quintero, M. Miranda, Mechanisms of photosensitization induced by drugs: a general survey. Ars Pharmaceutica **41**(1), 27–46 (2000)
18. S. Soldevila, M.C. Cuquerella, F. Bosca, Understanding of the photoallergic properties of fluoroquinolones: photoreactivity of lomefloxacin with amino acids and albumin. Chem. Res. Toxicol. **27**(4), 514–523 (2014). https://doi.org/10.1021/tx400377s
19. L.D. Saravolatz, J. Leggett, Gatifloxacin, gemifloxacin, and moxifloxacin: The role of 3 newer fluoroquinolones. Clin. Infect. Dis. **37**(9), 1210–1215 (2003). https://doi.org/10.1086/378809
20. I. Man, J. Murphy, J. Ferguson, Fluoroquinolone phototoxicity: a comparison of moxifloxacin and lomefloxacin in normal volunteers. J. Antimicrob. Chemother. **43**, 77–82 (1999). https://doi.org/10.1093/jac/43.suppl_2.77
21. H.S. Oliveira, M. Goncalo, A.C. Figueiredo, Photosensitivity to lomefloxacin. A clinical and photobiological study. Photodermatol. Photoimmunol. Photomed. **16**(3), 116–120 (2000). https://doi.org/10.1111/j.1600-0781.2000.160303.x
22. R. Dawe, J. Ferguson, S. Ibbotson et al., Lack of phototoxicity potential with delafloxacin in healthy male and female subjects: comparison to lomefloxacin. Photochem. Photobiol. Sci. **17**(6), 773–780 (2018). https://doi.org/10.1039/C8PP00019K
23. J.F. Zhao, Y.C. Liu, X.X. Jiang et al., Effect of C-5 position on the photochemical properties and phototoxicity of antofloxacin and levofloxacin: a stable and transient study. J. Photochem. Photobiol. B **155**, 122–129 (2016). https://doi.org/10.1016/j.jphotobiol.2015.12.004
24. J.F. Zhao, X.T. Zhang, R.X. Zhu et al., Photophysical properties controlled by substituents with lone-pair electrons at the ortho- or para-positions of fluoroquinolone antibiotics. J. Phys. Chem. B **123**(15), 3156–3162 (2019). https://doi.org/10.1021/acs.jpcb.8b10859
25. P. Perucca, M. Savio, O. Cazzalini et al., Structure-activity relationship and role of oxygen in the potential antitumour activity of fluoroquinolones in human epithelial cancer cells. J. Photochem. Photobiol. B **140**, 57–68 (2014). https://doi.org/10.1016/j.jphotobiol.2014.07.006
26. N. Hayashi, Y. Nakata, A. Yazaki, New findings on the structure-phototoxicity relationship and photostability of fluoroquinolones with various substituents at position 1. Antimicrob. Agents Chemother. **48**(3), 799–803 (2004). https://doi.org/10.1128/AAC.48.3.799-803.2004
27. H.X. Li, B.C. Zhou, Y.C. Liu et al., Primary photochemical properties of difloxacin in neutral aqueous solution. Acta Phys.-Chim. Sin. **30**(11), 2134–2141 (2014). https://doi.org/10.3866/PKU.WHXB201409161
28. J. Singh, A.K. Srivastva, P. Mandal et al., Under ambient UVA exposure, pefloxacin exhibits both immunomodulatory and genotoxic effects via multiple mechanisms. J. Photochem. Photobiol. B **178**, 593–605 (2018). https://doi.org/10.1016/j.jphotobiol.2017.12.014
29. V. Lhiaubet-Vallet, M.C. Cuquerella, J.V. Castell et al., Triplet excited fluoroquinolones as mediators for thymine cyclobutane dimer formation in DNA. J. Phys. Chem. B **111**(25), 7409–7414 (2007). https://doi.org/10.1021/jp070167f
30. L. Jian, W.-F. Wang, Z.-D. Zheng et al., Reactive intermediates in laser photolysis of guanosine. Res. Chem. Intermed. **15**(3), 293–301 (1991). https://doi.org/10.1163/156856791x00390
31. X. Li, J.-Q. Zhang, G.-Q. Lin et al., Performance of an electron linear accelerator for the first photoneutron source in China. Nucl. Sci. Tech. **30**(4), 53 (2019). https://doi.org/10.1007/s41365-019-0576-4
32. C. Feng, H.-X. Deng, Review of fully coherent free-electron lasers. Nucl. Sci. Tech. **29**(11), 160 (2018). https://doi.org/10.1007/s41365-018-0490-1
33. Z.-Y. Huang, K. Xuan, C.W. Li et al., Novel design of a personnel safety system for Hefei Light Source-II. Nucl. Sci. Tech. **30**(6), 99 (2019). https://doi.org/10.1007/s41365-019-0610-6
34. X.-D. Su, G.-L. Zhang, S.-P. Xu et al., Attenuation coefficients of gamma and X-rays passing through six materials. Nucl. Sci. Tech. **31**(1), 3 (2020). https://doi.org/10.1007/s41365-019-0717-9
35. S.D. Yao, S.G. Sheng, J.H. Cai et al., Nanosecond Pulse-Radiolysis Studies in China. Radiat. Phys. Chem. **46**(1), 105–109 (1995). https://doi.org/10.1016/0969-806X(94)00120-9
36. G.V. Buxton, C.L. Greenstock, W.P. Helman et al. Critical-review of rate constants for reactions of hydrated electrons, hydrogen-atoms and hydroxyl radicals (·OH/·O−) in aqueous-solution. J. Phys. Chem. Ref. Data **17**(2), 513–886 (1988). https://doi.org/10.1063/1.555805
37. J.F. Zhao, B.W. Zhang, C.H. Yu et al., Graphene oxide: A potential bodyguard protecting proteins from photosensitive damage. Carbon **109**, 487–494 (2016). https://doi.org/10.1016/j.carbon.2016.08.033
38. M. Frisch, G. Trucks, H. Schlegel et al., Gaussian 09; Gaussian, Inc. Wallingford, CT, **32**, 5648–5652 (2009)
39. P. Zhang, H.X. Li, S.D. Yao et al., Effects of pH and polarity on the excited states of norfloxacin and its 4'-*N*-acetyl derivative: a steady-state and time-resolved study. Sci. China Chem. **57**(3), 409–416 (2014). https://doi.org/10.1007/s11426-013-4986-6
40. K. Kawaoka, A. Khan, D.R. Kearns, Role of singlet excited states of molecular oxygen in the quenching of organic triplet states. J. Chem. Phys. **46**(5), 1842–1853 (1967). https://doi.org/10.1063/1.1840943
41. J. Vura-Weis, S.H. Abdelwahed, R. Shukla et al., Crossover from single-step tunneling to multistep hopping for molecular triplet energy transfer. Science **328**(5985), 1547–1550 (2010). https://doi.org/10.1126/science.1189354
42. I.M. Moller, B.K. Kristensen, Protein oxidation in plant mitochondria detected as oxidized tryptophan. Free Radic. Biol. Med. **40**(3), 430–435 (2006). https://doi.org/10.1016/j.freeradbiomed.2005.08.036
43. C.Y. Lu, W.Z. Lin, W.F. Wang et al., Riboflavin (VB2) photosensitized oxidation of 2 '-deoxyguanosine-5 '-monophosphate (dGMP) in aqueous solution: a transient intermediates study. Phys. Chem. Chem. Phys. **2**(3), 329–334 (2000). https://doi.org/10.1039/A908492D
44. I.G. Gut, P.D. Wood, R.W. Redmond, Interaction of triplet photosensitizers with nucleotides and DNA in aqueous solution at room temperature. J. Am. Chem. Soc. **118**(10), 2366–2373 (1996). https://doi.org/10.1021/ja9519344
45. O. Pandoli, A. Massi, A. Cavazzini et al., Circular dichroism and UV–Vis absorption spectroscopic monitoring of production of chiral silver nanoparticles templated by guanosine 5'-monophosphate. Analyst **136**(18), 3713–3719 (2011). https://doi.org/10.1039/C1AN15288B
46. S.V. Jovanovic, M.G. Simic, The DNA guanyl radical - kinetics and mechanisms of generation and repair. Biochim. Biophys. Acta. **1008**(1), 39–44 (1989). https://doi.org/10.1016/0167-4781(89)90167-X
47. M.B. Feng, Z.Y. Wang, D.D. Dionysiou et al., Metal-mediated oxidation of fluoroquinolone antibiotics in water: a review on kinetics, transformation products, and toxicity assessment. J. Hazard. Mater. **344**, 1136–1154 (2018). https://doi.org/10.1016/j.jhazmat.2017.08.067

48. L. Wojnarovits, T. Toth, E. Takacs, Critical evaluation of rate coefficients for hydroxyl radical reactions with antibiotics: a review. Crit. Rev. Environ. Sci. Technol. **48**(6), 575–613 (2018). https://doi.org/10.1080/10643389.2018.1463066
49. L.M. Dorfman, G.E. Adams, Reactivity of the hydroxyl radical in aqueous solutions; National Standard Reference Data System: 1973 (1973)
50. R. Cegielska-Radziejewska, G. Lesnierowski, T. Szablewski et al., Physico-chemical properties and antibacterial activity of modified egg white-lysozyme. J. Eur. Food Res. Technol. **231**(6), 959–964 (2010). https://doi.org/10.1007/s00217-010-1347-y
51. V. Paviani, R.F. Queiroz, E.F. Marques et al., Production of lysozyme and lysozyme-superoxide dismutase dimers bound by a ditryptophan cross-link in carbonate radical-treated lysozyme. Free Radic. Biol. Med. **89**, 72–82 (2015). https://doi.org/10.1016/j.freeradbiomed.2015.07.015
52. E. Fuentes-Lemus, M. Mariotti, P. Hägglund et al., Binding of rose bengal to lysozyme modulates photooxidation and cross-linking reactions involving tyrosine and tryptophan. Free Radic. Biol. Med. **143**, 375–386 (2019). https://doi.org/10.1016/j.freeradbiomed.2019.08.023
53. L. Carroll, D.I. Pattison, J.B. Davies et al., Formation and detection of oxidant-generated tryptophan dimers in peptides and proteins. Free Radic. Biol. Med. **113**, 132–142 (2017). https://doi.org/10.1016/j.freeradbiomed.2017.09.020
54. L.J. Martinez, R.H. Sik, C.F. Chignell, Fluoroquinolone antimicrobials: singlet oxygen, superoxide and phototoxicity. Photochem. Photobiol. **67**(4), 399–403 (1998). https://doi.org/10.1111/j.1751-1097.1998.tb05217.x
55. A. Kawada, K. Hatanaka, H. Gomi, In vitro phototoxicity of new quinolones: production of active oxygen species and photosensitized lipid peroxidation. Photodermatol. Photoimmunol. Photomed. **15**(6), 226–230 (1999). https://doi.org/10.1111/j.1600-0781.1999.tb00094.x
56. L.I. Grossweiner, A.S. Patel, J.B. Grossweiner, Type-I and Type-II mechanisms in the photosensitized lysis of phosphatidylcholine liposomes by hematoporphyrin. Photochem. Photobiol. **36**(2), 159–167 (1982). https://doi.org/10.1111/j.1751-1097.1982.tb04358.x
57. C.S. Foote, Definition of Type-I and Type-II photosensitized oxidation. Photochem. Photobiol. **54**(5), 659–659 (1991). https://doi.org/10.1111/j.1751-1097.1991.tb02071.x
58. L. Ge, J. Chen, X. Wei et al., Aquatic photochemistry of fluoroquinolone antibiotics: kinetics, pathways, and multivariate effects of main water constituents. Environ. Sci. Technol. **44**(7), 2400–2405 (2010). https://doi.org/10.1021/es902852v
59. G. de Guidi, G. Bracchitta, A. Catalfo, Photosensitization reactions of fluoroquinolones and their biological consequences. Photochem. Photobiol. **87**(6), 1214–1229 (2011)
60. A. Albini, S. Monti, Photophysics and photochemistry of fluoroquinolones. Chem. Soc. Rev. **32**(4), 238–250 (2003). https://doi.org/10.1039/B209220B
61. S.Y. Xie, J.F. Zhao, B.W. Zhang et al., Graphene oxide transparent hybrid film and its ultraviolet shielding property. ACS Appl. Mater. Interfaces **7**(32), 17558–17564 (2015). https://doi.org/10.1021/acsami.5b04231
62. Y. Hachimori, K. Kurihara, K. Shibata et al., States of amino acid residues in proteins. V. Different reactivities with H_2O_2 of tryptophan residues in lysozyme proteinases and zymogens. Biochim. Biophys. Acta **93**(2), 346–360 (1964). https://doi.org/10.1016/0304-4165(64)90385-X
63. P. Bilski, L.J. Martinez, E.B. Koker et al., Photosensitization by norfloxacin is a function of pH. Photochem. Photobiol. **64**(3), 496–500 (1996). https://doi.org/10.1111/j.1751-1097.1996.tb03096.x
64. F. Lorenzo, S. Navaratnam, R. Edge et al., Primary photoprocesses in a fluoroquinolone antibiotic sarafloxacin. Photochem. Photobiol. **85**(4), 886–894 (2009). https://doi.org/10.1111/j.1751-1097.2009.00553.x
65. Y. Zelmat, V. Rousseau, L. Chebane et al., Fluoroquinolone-induced photosensitivity: a chemical fragment-based approach by a case/non-case study in VigiBase®. Drug Saf. (2020). https://doi.org/10.1007/s40264-020-00917-4